Article

Developmental Cell

Cell-Cycle Proteins Control Production of Neutrophil Extracellular Traps

Highlights

- Neutrophils activate cell-cycle markers when stimulated to make NETs
- Cyclin-dependent kinases CDK4/6 regulate NET formation
- Cdk6$^{-/-}$ mice have impaired immune response to *Candida albicans*

Authors

Borko Amulic, Sebastian Lorenz Knackstedt, Ulrike Abu Abed, ..., Frank L. Heppner, Philip W. Hinds, Arturo Zychlinsky

Correspondence

zychlinsky@mpiib-berlin.mpg.de

In Brief

Neutrophils release chromatin in the form of neutrophil extracellular traps (NETs). Amulic et al. show that NET formation involves activation of cell-cycle markers and identify CDK4/6 as regulators of the process. Cdk6 knockout mice, which are impaired in NET formation, are more susceptible to *Candida albicans* infection.

Amulic et al., 2017, Developmental Cell *43*, 449–462
November 20, 2017
https://doi.org/10.1016/j.devcel.2017.10.013

CellPress

Developmental Cell
Article

Cell-Cycle Proteins Control Production of Neutrophil Extracellular Traps

Borko Amulic,[1] Sebastian Lorenz Knackstedt,[1] Ulrike Abu Abed,[1,2] Nikolaus Deigendesch,[1,3] Christopher J. Harbort,[1] Brian E. Caffrey,[4] Volker Brinkmann,[2] Frank L. Heppner,[3,5,6,7] Philip W. Hinds,[8] and Arturo Zychlinsky[1,9,*]
[1]Department of Cellular Microbiology, Max Planck Institute for Infection Biology, Berlin 10117, Germany
[2]Microscopy Core Facility, Max Planck Institute for Infection Biology, Berlin 10117, Germany
[3]Department of Neuropathology, Charité - Universitätsmedizin, 10117 Berlin, Germany
[4]Max Planck Institute for Molecular Genetics, 14195 Berlin, Germany
[5]Cluster of Excellence, NeuroCure, 10117 Berlin, Germany
[6]Berlin Institute of Health (BIH), 10178 Berlin, Germany
[7]German Center for Neurodegenerative Diseases (DZNE) Berlin, 10117 Berlin, Germany
[8]Department of Developmental, Molecular and Chemical Biology, Tufts University School of Medicine, Boston, MA 02111, USA
[9]Lead Contact
*Correspondence: zychlinsky@mpiib-berlin.mpg.de
https://doi.org/10.1016/j.devcel.2017.10.013

SUMMARY

Neutrophils are essential for immune defense and can respond to infection by releasing chromatin in the form of neutrophil extracellular traps (NETs). Here we show that NETs are induced by mitogens and accompanied by induction of cell-cycle markers, including phosphorylation of the retinoblastoma protein and lamins, nuclear envelope breakdown, and duplication of centrosomes. We identify cyclin-dependent kinases 4 and 6 (CDK4/6) as essential regulators of NETs and show that the response is inhibited by the cell-cycle inhibitor $p21^{Cip}$. CDK6, in neutrophils, is required for clearance of the fungal pathogen *Candida albicans*. Our data describe a function for CDK4/6 in immunity.

INTRODUCTION

Neutrophils are the most abundant immune cells in the bloodstream. They are essential for survival; in humans a lack of neutrophils results in severe immunodeficiency and a drastically reduced lifespan, as for example in individuals with mutations causing congenital neutropenias (Klein, 2011). Neutrophils are produced in the bone marrow from dividing progenitors. After maturing and exiting the cell cycle they move to the circulatory system where they are thought to have a short lifespan. Upon infection or injury they migrate into affected tissues where they directly kill pathogens, as well as shaping the ensuing adaptive immune response (Amulic et al., 2012; Mantovani et al., 2011).

Neutrophils kill microbes by phagocytosis, production of reactive oxygen species (ROS), and by release of various microbicidal proteins. Before activation, these antimicrobials are kept in intracellular storage vesicles called granules. When the cell senses pathogens, the antimicrobials can be released by a process called degranulation, whereby the granules fuse with the plasma membrane and release their contents. An additional antimicrobial strategy has been described, which entraps pathogens in neutrophil extracellular traps (NETs) (Brinkmann et al., 2004). These consist of extruded chromatin bound to various antimicrobials from the granules. By associating with NETs, the antimicrobial molecules are physically limited from diffusing away from their site of action, which may enhance their killing capacity, as well as limit collateral damage to host tissues. NETs are triggered by large pathogens, such as hyphal forms of *Candida albicans* (Branzk et al., 2014). Furthermore, excessive NET release is associated with a growing list of inflammatory and autoimmune diseases, including systemic lupus erythematosus (SLE) (Kaplan and Radic, 2012), atherosclerosis (Warnatsch et al., 2015), diabetes (Wong et al., 2015), vasculitis (Kaplan and Radic, 2012), thrombosis (Martinod and Wagner, 2014), sepsis (Camicia et al., 2014), and cancer (Park et al., 2016). Understanding the molecular mechanism of NET formation is thus crucial for developing therapeutics in the context of immune defense and inflammatory diseases.

NETosis is a type of neutrophil cell death, distinct from apoptosis or necrosis, which remains poorly characterized. It is an active process characterized by internal breakdown of nuclear and granular membranes, the mixing of the contents of these compartments in the cytosol and finally, their extracellular release via plasma membrane rupture (Fuchs et al., 2007). Although alternative pathways have been reported (Park et al., 2016; Parker et al., 2012; Kenny et al., 2017), the most studied NETosis program is the one in response to *C. albicans* and the mitogen phorbol myristate acetate (PMA). It requires signaling through mitogen-activated protein kinases (MAPKs) (Hakkim et al., 2011) and the production of ROS by the enzyme NADPH oxidase (NOX2) (Fuchs et al., 2007). ROS are required for the permeabilization of granules by a protein complex called the azurosome, which allows translocation of a protease, neutrophil elastase, into the nucleus where it cleaves histones and leads to chromatin decondensation (Papayannopoulos et al., 2010; Metzler et al., 2014). Other mechanistic aspects remain unknown, although some forms of NET formation are associated with citrullination of histones, catalyzed by the enzyme protein arginine deiminase 4 (PAD4) (Li et al., 2010; Kenny et al., 2017).

One of the most distinctive features of NETosis is the breakdown of the nuclear envelope. This characteristic sets it apart from apoptosis, and is highly reminiscent of nuclear envelope disintegration during mitosis in dividing cells. This observation led us to postulate that NET induction is linked to mitogenic reactivation of cell-cycle regulators. We show that neutrophils, which are terminally differentiated cells, upregulate Ki-67, phosphorylate retinoblastoma protein (pRb), and nuclear lamins, and separate centrosomes without replicating DNA or undergoing cytokinesis. We demonstrate that core members of the cell-cycle machinery, cyclin-dependent kinases 4 and 6 (CDK4/6), are required for NET formation. Taken together, the data presented here show that, in neutrophils, cell-cycle pathways are repurposed for controlling NETosis.

RESULTS

Mitogens Induce NETs

Fungi and the protein kinase C agonist PMA activate a similar pathway to make NETs. Both induce MAPK signaling (Hakkim et al., 2011), the activation of NOX2, and the production of ROS (Fuchs et al., 2007). PMA is also a strong mitogen, a chemical with the ability to trigger cell division. We tested if other mitogens also lead to NET release. Concanavalin A (ConA) and phytohaemagglutinin, two plant lectins commonly used to induce proliferation of lymphocytes, both induced NETs, distinguishable by their morphology and the colocalization of nuclear and granular markers (Figures 1A and 1B). Importantly, NET induction with mitogens was also dependent on ROS production, since neutrophils isolated from chronic granulomatous disease (CGD) patients, who have deficiencies in NOX2, or those treated with diphenyleneiodonium, a NOX2 chemical inhibitor, did not undergo NETosis (Figures 1A and 1B).

NETosis Is Accompanied by Induction of Cell Division Markers

Neutrophils are terminally differentiated cells that have withdrawn from the cell cycle and lost their capacity to divide. Indeed, mature neutrophils downregulate most of the genes involved in cell-cycle regulation (Klausen et al., 2004), a finding we confirmed by genome-wide expression analysis of peripheral blood neutrophils from healthy donors (Table S1). Despite this, mitogenic stimulation of neutrophils leads to nuclear envelope breakdown as it does in the case of mitosis in dividing cells. Transmission electron microscopy comparing mitosis in the myeloid cell line PLB-985, and NETosis in neutrophils, revealed that the vesiculation of the nuclear envelope is common to both processes (Figure 1C; Fuchs et al., 2007). We were struck by this similarity and postulated that common cellular pathways are employed during NETosis and mitosis.

We first examined cell-cycle markers in neutrophils induced to make NETs. The nuclear antigen Ki-67 is expressed in all cycling cells, irrespective of the stage of the cell cycle they are in, while it is absent in non-cycling, quiescent, or senescent cells. Resting neutrophils were negative for Ki-67 but, surprisingly, cells stimulated to undergo NETosis transiently reactivated expression of this cell division marker, visualized by immunofluorescence (Figures 2A and 2B).

We examined a series of other cell-cycle markers, in the order in which they are induced in dividing cells. Neutrophils are typically considered to be in the G_0 stage, like other terminally differentiated and quiescent cells (Figure S1). Cells in G_0 can resume cycling after mitogenic stimulation; this is associated with phosphorylation of pRb by CDK4/6 (Malumbres and Barbacid, 2009). Notably, neutrophils stimulated to make NETs also exhibited robust phosphorylation of pRb, indicating that activation of G1 kinases was occurring (Figure 2C). Importantly, pRb phosphorylation was not only triggered by PMA and ConA, but also by infection with *C. albicans* hyphae (Figure 2C). Stimuli that activate neutrophils but do not induce NETs, such as bacterial peptide analog N-formylmethionyl-leucyl-phenylalanine (fMLP), did not lead to pRb phosphorylation.

Despite activation of G1 kinases, we did not detect incorporation of the thymidine analog 5-ethynyl-2′-deoxyuridine (EdU) (Figure 2D), indicating that DNA synthesis, the hallmark of S phase, did not occur. As a control for EdU incorporation we used continuously cycling HEK293 cells (Figure 2D) as well as T lymphocytes, which can be induced to proliferate by treatment with PMA, analogously to our stimulation of neutrophils. T cells stimulated with PMA/ionomycin successfully incorporated EdU, but this required a longer period of stimulation than the 3 hr it took neutrophils to make NETs (Figure S1B), highlighting an important difference in the temporal dynamic between NETosis and cell-cycle re-entry. Similarly, we observed no induction of the S-phase transcriptional program in neutrophils making NETs. In cycling cells, phosphorylation of pRb leads to the derepression of E2F transcription factors and expression of S-phase genes, but these were not induced in NETosis as measured by qPCR analysis (Figure S1C) and whole-genome microarray analysis (data not shown).

Our initial observation of nuclear envelope breakdown during NETosis (Figure 1C) argued that mitotic pathways are also activated. In mitosis (M phase), nuclear envelope disintegration is triggered by phosphorylation of lamins, intermediate filament proteins that form a sheet underneath the envelope called the nuclear lamina (Heald and McKeon, 1990). Phosphorylation of the lamina disrupts the structural rigidity of the nucleus, allowing the nuclear envelope to disintegrate. We tested if NET formation is also associated with phosphorylation of lamins. Remarkably, treatment with the NET-inducing stimuli PMA, ConA, or *C. albicans* hyphae all led to robust phosphorylation of lamin A/C (Figure 2C). This was confirmed by immunofluorescence (Figures S1D and S1E). Furthermore, NETosis was accompanied by induction of a second mitotic marker: phosphorylation of histone H3 at serine 10 (H3S10). Neither lamin nor H3S10 phosphorylation were induced by the control stimulus fMLP (Figure 2C), which, as mentioned above, does not induce NETs.

Induction of NETs Leads to Centrosome Separation

To test whether NET formation involves induction of other mitotic markers, we visualized microtubule dynamics by immunofluorescence microscopy. During mitosis, microtubule-based structures called centrosomes, which were duplicated in the preceding S phase, separate and migrate to opposing poles of the cell where they nucleate formation of the mitotic spindle (Mardin and Schiebel, 2012). In unstimulated neutrophils, immunostaining with an antibody directed against both α- and

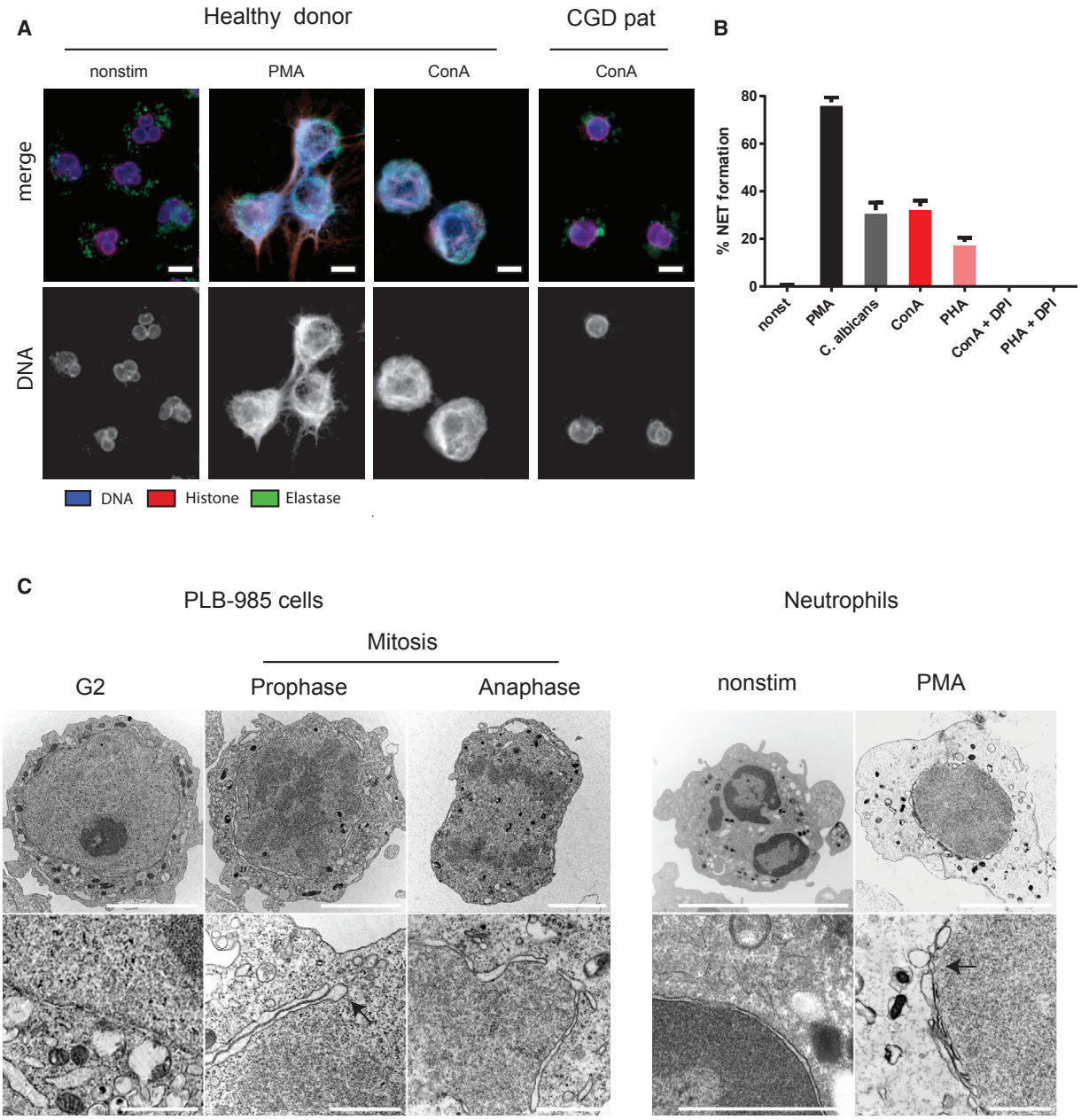

Figure 1. Mitogens Induce NETs

(A) Human peripheral blood neutrophils isolated from a healthy donor or CGD patient (n = 2) with a genetic deficiency in NOX2, stimulated with PMA (50 nM) or ConA (50 μg/mL) for 5 hr. Both stimuli lead to colocalization of chromatin (red), DNA (blue), and the granule protein neutrophil elastase (green). Representative image from three independent experiments. Nonstim, nonstimulated. Top row, merge; bottom row, DNA. Scale bars, 5 μm.

(B) Quantification of NET induction with mitogens and *C. albicans,* and inhibition with the NOX2 inhibitor diphenyliodonium (DPI, 5 μM). Representative result of three independent repeats, means ± SD.

(C) Electron micrograph comparing nuclear envelope breakdown in mitosis and NETosis. Left: PLB-985 cells were synchronized in G2 and then released into mitosis. In G2 the nuclear envelope is intact but disintegrates in the prophase of mitosis, concurrently with appearance of condensed chromosomes (darker staining territories in the nucleus). In anaphase, chromosomes have separated and, eventually the nuclear envelope begins to reform. Right: nonstimulated neutrophils have a lobulated nucleus, but this lobulation is lost as they prepare to release NETs. Approximately 2 hr after PMA stimulation, the nuclear envelope starts to disintegrate, allowing nuclear material to mix with the contents of the granules and the cytoplasm before being released into the extracellular space. The bottom row shows magnified details from corresponding top panels. Arrows indicate vesiculation of the nuclear envelope. Neutrophil images are representative from at least five different embeddings. Scale bars, 5 μm (upper panels; overview) and 1 μm (lower panels; detailed views).

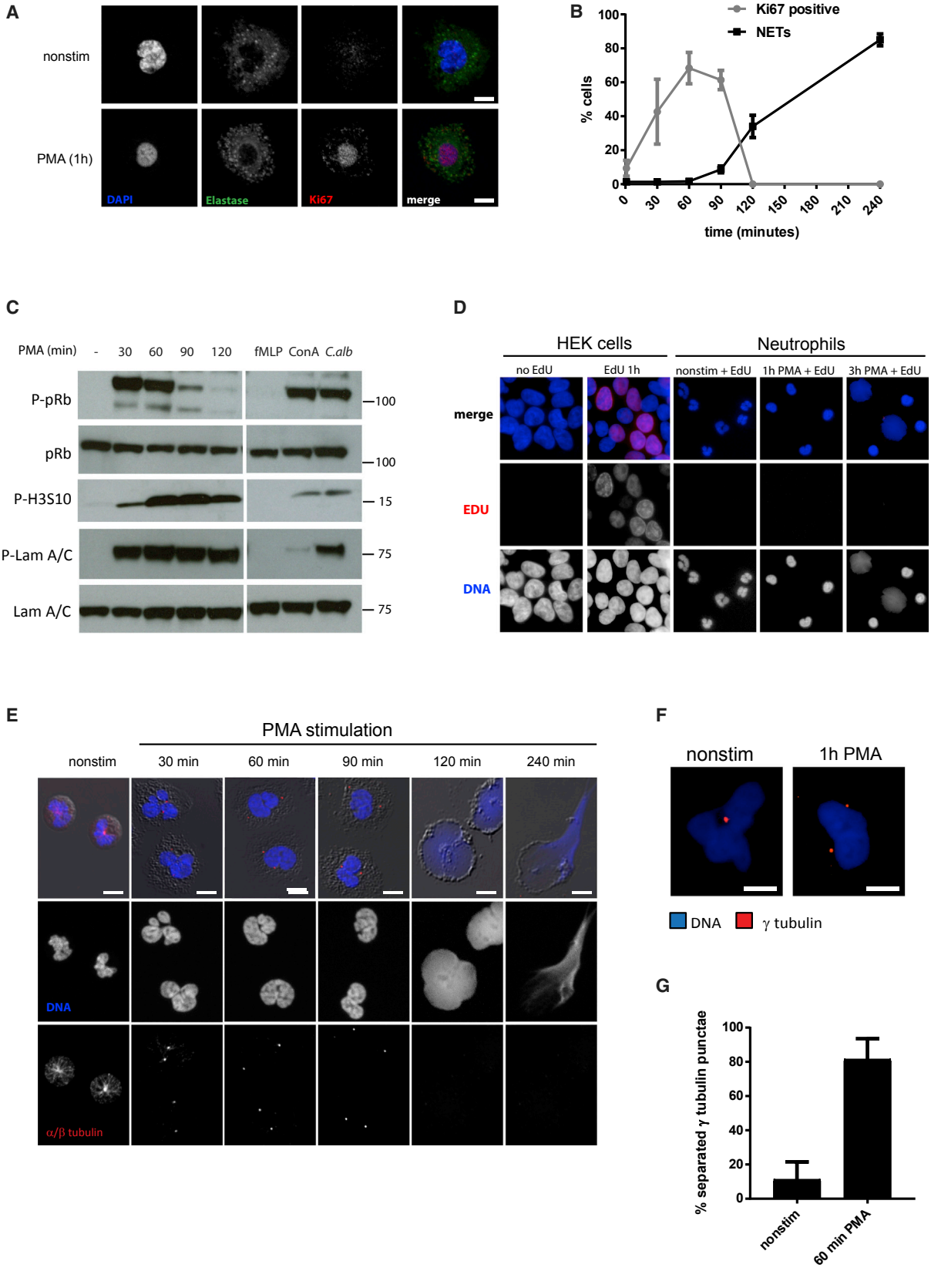

(legend on next page)

β-tubulin demonstrated a "skeletal" or scaffold-like staining pattern with several filaments extending from a central microtubule-organizing center (Figures 2E and S1F). After 30 min of PMA stimulation these extended filaments were lost and rearranged into single or double dot-like structures. Strikingly, 60 min post-stimulation, these dot-like structures had duplicated and migrated away from each other. The structures were most fully separated from each other at 90 min post-stimulation and were no longer present by 120 min, which coincided with breakdown of the nuclear envelope. Immunofluorescence detection of the centrosome marker γ-tubulin confirmed that these structures were *bona fide* centrosomes (Figures 2F and 2G). Treatment with the control stimulus fMLP did not induce microtubule rearrangement (Figure S1G). Centrosome separation, together with phosphorylation of lamins and histone H3S10, demonstrate that markers of a mitotic program are present just before neutrophils die and release NETs.

Neutrophils Activate Cell-Cycle Signaling *In Vivo*

Induction of cell-cycle markers in neutrophils was surprising since they are terminally differentiated cells. To verify that this also occurs *in vivo*, we induced NETs by inoculating mice with *C. albicans* via the orotracheal route. We then co-stained lung sections with antibodies against neutrophil markers (calgranulin A or Ly6G) and the cell division marker Ki-67. Interestingly, we identified many Ki-67-positive neutrophils in the infected lungs (Figures 3A and S2A).

We also examined human histological sections from patients with brain fungal abscesses, identified by periodic acid-Schiff staining (Figure S2B). We observed NETs in these sections by detecting neutrophil elastase co-localizing with DNA (Figure S2C). Next, we co-stained sections with Ki-67 and the neutrophil marker calgranulin, and indeed were able to observe Ki-67-positive neutrophil infiltrates (Figure 3B). We confirmed this finding using immunohistochemical methods with a second Ki-67 antibody (Figure S2D), as well as immunofluorescent-based detection of a second neutrophil marker (CD66b; Figure S2E). Neutrophils were only Ki-67 positive when they had intact nuclei (NET precursors), as was the case with Ki-67 detection in purified neutrophils (Figure 2B). Remarkably, we could also detect duplicated centrosomes in these cells (Figure 3C), demonstrating the induction of mitotic pathways in neutrophils *in vivo* and confirming our results with isolated human cells.

The Cell-Cycle Inhibitor $p21^{cip}$ Regulates NET Formation

Human neutrophils are refractory to transfection and gene editing because of their short lifespans. As an initial approach to determine whether NETosis is dependent on the cell cycle, we used cell-penetrating peptides. In dividing cells, one class of negative cell-cycle regulators is a family of small proteins termed cip/kip (*CDK interacting protein/Kinase inhibitory protein*). The prototype of this family is $p21^{cip1}$ (p21), a protein that blocks the cell cycle at several different points (Figure S1A) by inhibiting cyclin-CDK complexes. We synthesized a peptide mimic corresponding to the CDK inhibitory domain of p21 (Rousseau et al., 1999), which was previously shown to inhibit proliferation by interfering with the activity of CDKs. We coupled this peptide to the cell-penetrating *tat* sequence (Goulvestre et al., 2005). A scrambled peptide served as the control. Both peptides penetrated neutrophils with similar efficiencies (Figure S3A), and neither were toxic to the cells (Figure S3B). Transduction of the p21 inhibitory peptide (p21inh) into human neutrophils completely blocked NET formation, while transduction of the control scrambled peptide (p21ctrl) had little effect (Figures 4A and 4B). Interference with CDKs thus leads to inhibition of NET release, indicating that these cell-cycle regulators are necessary for NETosis. We also examined NET formation in p21 knockout mice, whose cells have higher proliferative capacities due to increased CDK activity and loss of cell-cycle control (Bedelbaeva et al., 2010). As expected, peritoneal neutrophils from p21 knockout mice made more NETs than wild-type (WT) cells (Figure 4C), consistent with p21 being a regulator of both cell-cycle and NET formation. ROS production, however, was similar in both strains (Figure 4D).

Neutrophils Express CDK4/6

The early stages of NET formation display various cell-cycle markers and can be blocked by the CDK binding domain of the p21 cell-cycle inhibitor. CDKs and their regulatory subunits, the cyclins, are the major drivers of the mammalian cell cycle (Figure S1A). The CDKs are a large group of kinases, many of which have functions unrelated to the cell cycle (Lim and Kaldis, 2013). Of the canonical cell-cycle regulatory kinases, the close homologs CDKs 4 and 6 regulate the transition from G_0 to G_1 phase and are considered to be largely redundant (Malumbres and Barbacid, 2009). CDK2 drives progression through S phase, while CDK1 is essential for mitosis, although much functional

Figure 2. NET Formation Is Associated with Induction of Cell-Cycle Markers

(A) Nonstimulated (nonstim, top panel) and PMA-treated human neutrophils stained for Ki-67 (red) and elastase (green). Representative image from four different experiments. Scale bars, 5 μm.

(B) Quantification of nuclear Ki-67 staining during PMA time course stimulation. The percentage of Ki67-positive cells (gray) is plotted along with the percentage of SYTOX-positive cells (black). The graph shows means ± SEM from combined data of four healthy donors.

(C) Western blot of G1/S and M phase markers in lysates prepared from human neutrophils simulated with NET inducers (PMA, ConA, and *C. albicans*) and a control stimulus that does not induce NETs (fMLP). "P-" indicates phosphorylation. Representative blot from three or more repeats with different donors. Molecular weights are indicated in kDa.

(D) Immunofluorescence analysis of EdU incorporation in control HEK cells (left) and human neutrophils making NETs (right). Neutrophils were incubated with nucleotide analog EdU for 1 hr before PMA stimulation and were then fixed at indicated times. HEK cells (nonstimulated) were incubated with EdU or vehicle control for 1 hr before fixing.

(E) Immunofluorescence detection of microtubules with an antibody against α- and β-tubulin (red), in a time course experiment of human neutrophils stimulated with PMA.

(F) Nonstimulated and PMA-treated (1 hr) human neutrophils stained for γ-tubulin (red) and DNA (blue). (E and F) Representative images from three different independent experiments, with cells from different donors. Scale bars 5 μm.

(G) Quantification of separated centrosomes from (F). Graph shows means ± SEM from combined data of four donors. See also Figure S1.

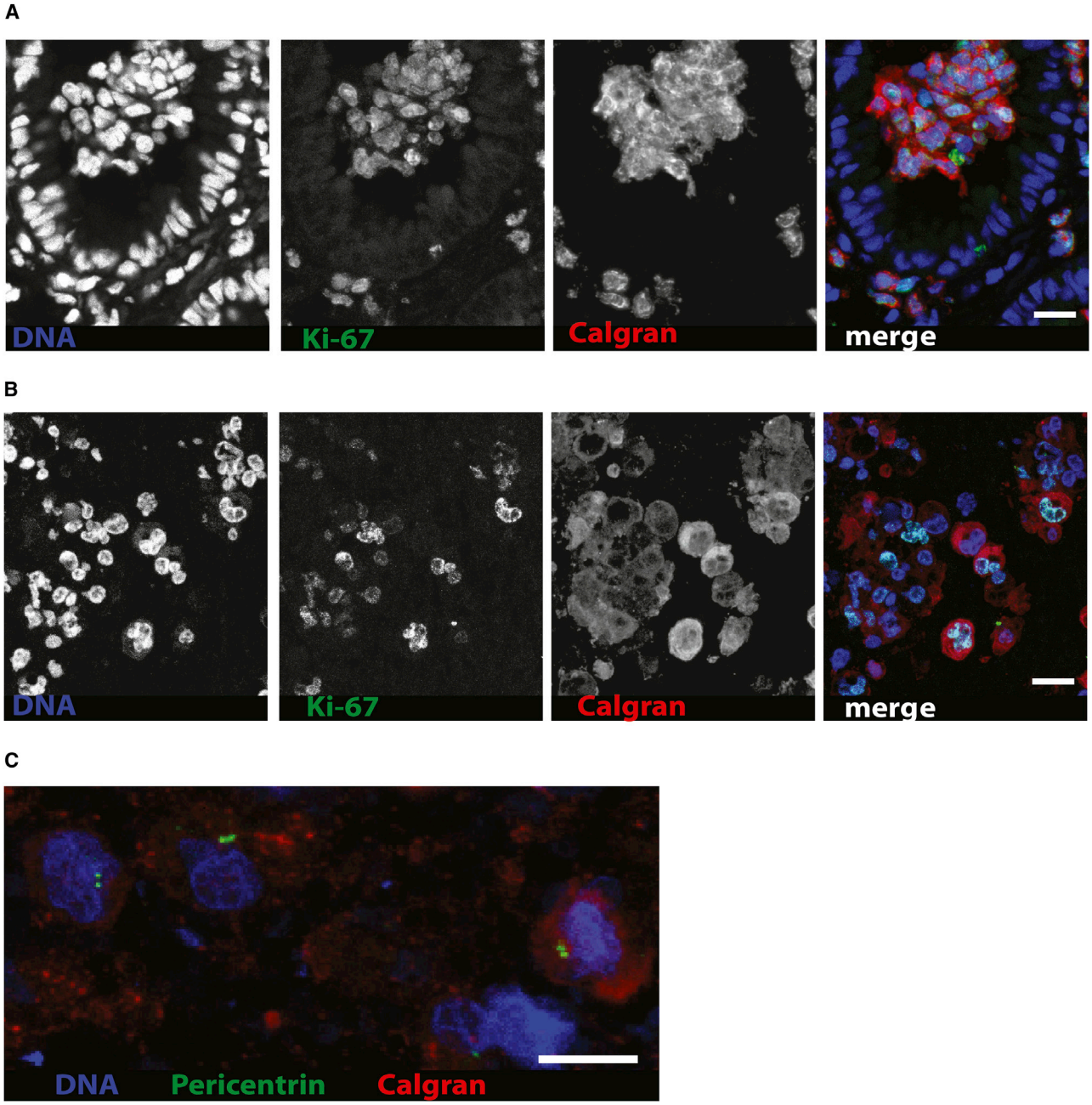

Figure 3. Neutrophils Activate Cell-Cycle Signaling *In Vivo*

(A and B) Immunostaining of mouse lung infected with *C. albicans* (A) or human brain fungal abscess (B) showing neutrophils labeled with calgranulin (red) expressing Ki-67 (green) in the nucleus. Representative image from six mice or four different human specimens.

(C) Neutrophils (red/calgranulin) in human brain fungal abscess, showing duplicated and separated centrosomes (green). (A–C) Blue, DNA. Scale bars, 10 μm. See also Figure S2.

overlap has been reported (Figure S1A; Malumbres and Barbacid, 2009). We examined protein expression of the cell-cycle CDKs in human neutrophils and were able to detect CDK4/6 (Figure 5A). CDK4 was present at the protein level, as well as induced at the transcriptional level, after NET induction (Figure S4A), while CDK6 was only present at the protein level (Figure 5A). Neutrophils did not express CDK2 or CDK1 (Figures 5A and S4A), in agreement with previous reports (Leitch et al., 2012; Klausen et al., 2004).

CDK4/6 are implicated in phosphorylation of pRb (Meyerson and Harlow, 1994) and in centrosome separation (Hussain et al., 2013) both of which occur during NET formation (Figures 2C and 2F). Furthermore, CDK4/6 activity can be induced via MAPK signaling and is a central link between extracellular

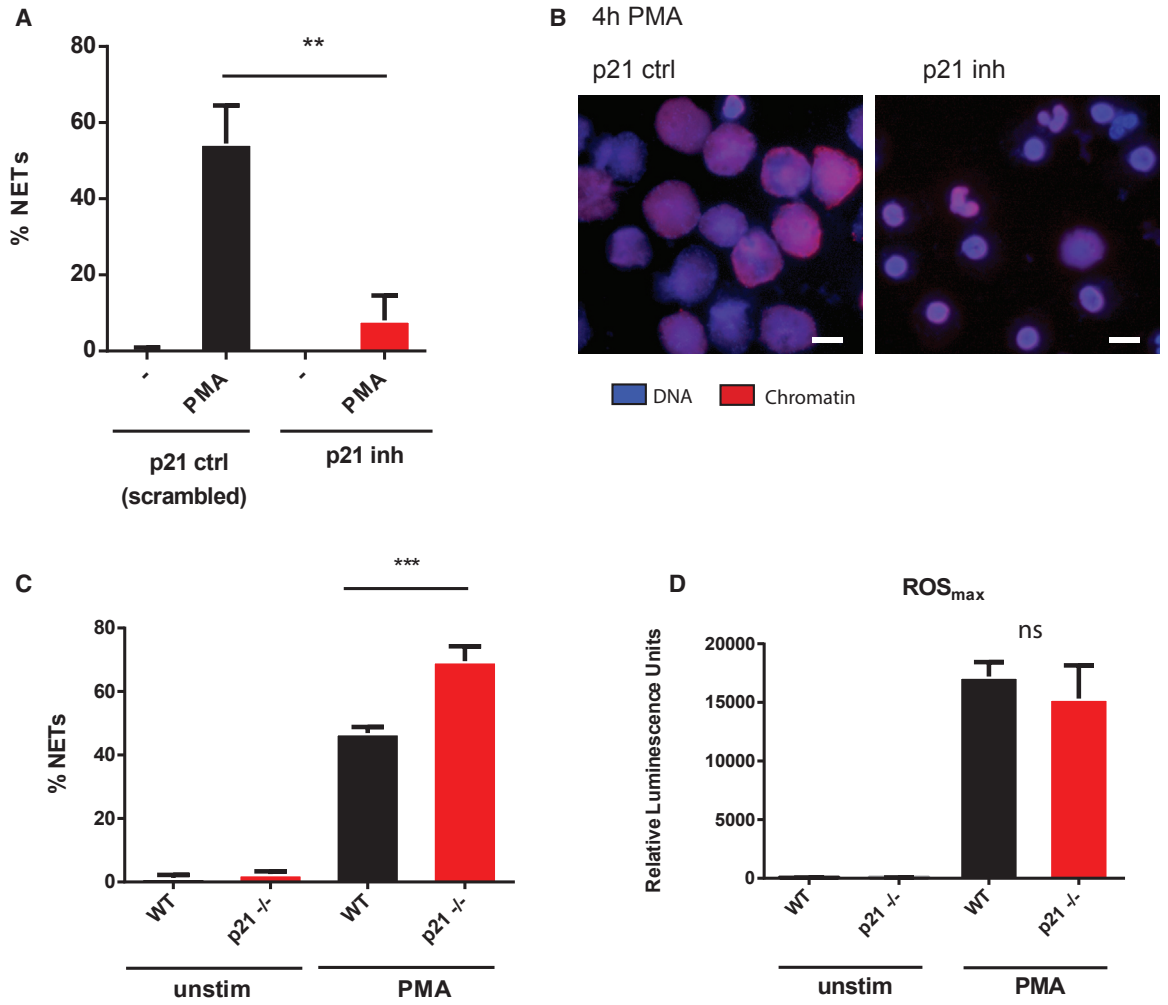

Figure 4. p21 Regulates NETs

(A) Human neutrophils were incubated with a peptide corresponding to the CDK inhibitory domain of the p21 protein (p21inh), or a scrambled control peptide (p21ctrl), at a concentration of 20 μM before activation of NETs with PMA. The graph shows means ± SEM of NET formation after 4 hr. n = 3 donors. **$p < 0.01$, unpaired Student's t test.

(B) Representative immunofluorescence images of PMA-stimulated cells pre-incubated with p21 peptide or scrambled control, from three independent repeats. DNA is shown in blue and chromatin in red. Scale bars, 10 μm.

(C) NET formation in WT and $p21^{-/-}$ mouse peritoneal neutrophils after 5 hr of PMA stimulation. Bars show means ± SEM, n = 4 mice. ***$p < 0.001$, unpaired Student's t test.

(D) Oxidative burst in WT and $p21^{-/-}$ mouse peritoneal neutrophils in response to PMA. Bars show means of maximum luminescence intensity, ± SEM. n = 4; ns, non-significant, unpaired Student's t test. See also Figure S3.

growth signals and induction of proliferation (Malumbres and Barbacid, 2009). CDK6 localizes throughout the cytoplasm in unstimulated neutrophils and transiently accumulates in the nucleus of PMA-stimulated cells (Figure 5B). We could not determine the localization of CDK4. Neutrophils express the CDK4/6 regulatory co-factor cyclin D2 and low levels of cyclin D3 (Figure 5C).

CDK4/6 Controls NET Formation

To test if these G1 kinases are involved in NET formation, we incubated human neutrophils with a CDK4/6 pharmacological inhibitor (abemaciclib/LY2835219), which efficiently blocked NETs in a dose-dependent manner (Figures 5D, S4D, and S4E), but did not inhibit the oxidative burst (Figure 5F), phagocytosis (Figure 5G), or degranulation (Figure S4F). This was confirmed with a second Cdk4/6 inhibitor (palbociclib, Figure 5E). Both inhibitors blocked ConA-induced NETs at lower concentrations than those required for PMA, consistent with ConA being a weaker stimulus. CDK4/6 inhibition blocked translocation of elastase to the nucleus (Figure S4G), a requirement for NET release (Papayannopoulos et al., 2010).

CDK4/6 double knockout mice die at late stages of embryonic development due to severe anemia (Malumbres et al., 2004). The kinases have, however, been knocked out individually. Cdk6 knockout mice are viable and have only mild hematopoietic disturbances (Malumbres et al., 2004; Hu et al., 2009). We used a

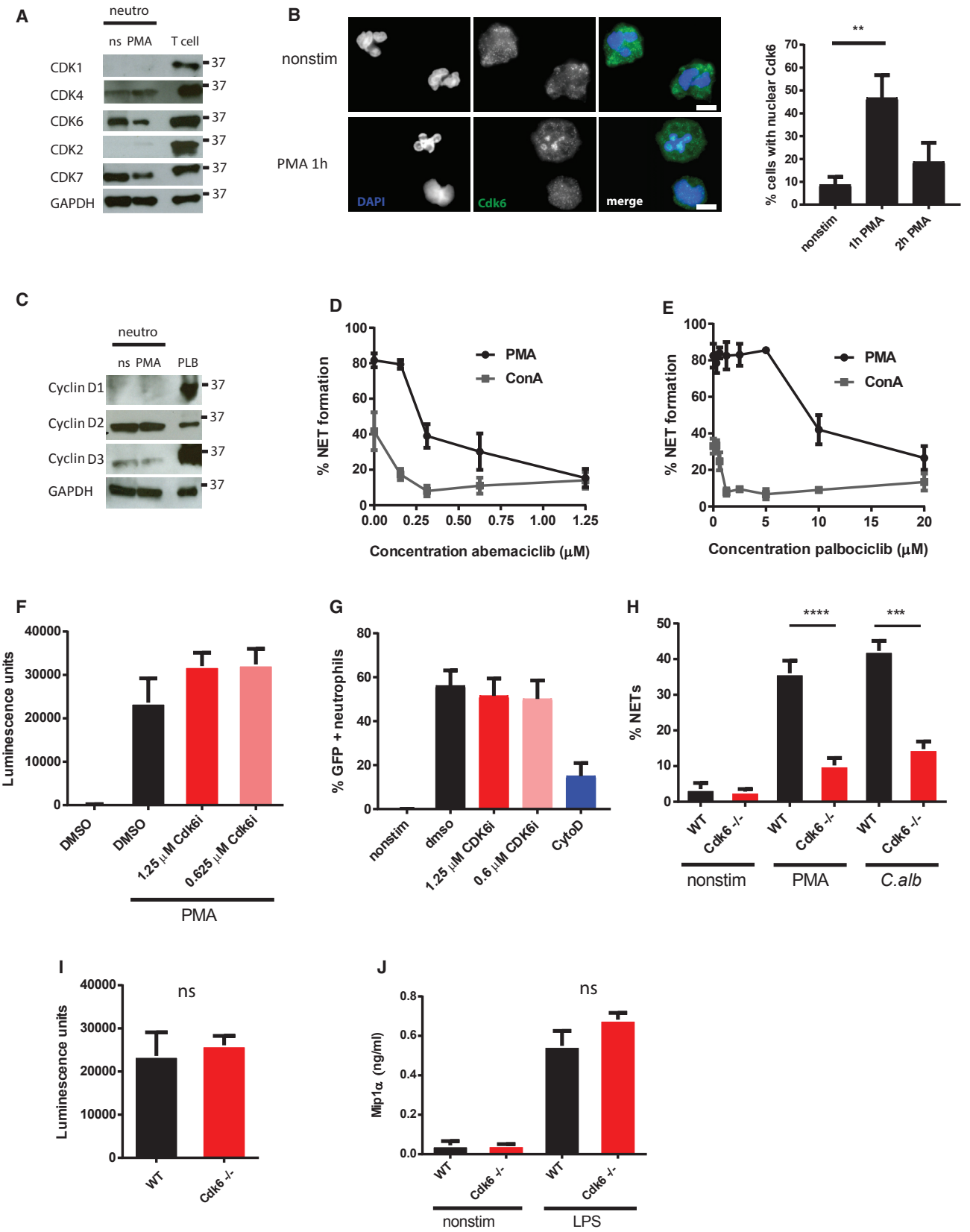

(legend on next page)

Cdk6$^{-/-}$ mouse strain in which expression of the gene was interrupted by insertion of a floxed transcriptional stop cassette in the first exon (Hu et al., 2009). We purified neutrophils from the peritoneum of Cdk6$^{-/-}$ and WT mice (Figure S5A) and obtained similar yields and purities (Figure S5B). Like human neutrophils, mouse neutrophils expressed Cdk4 as well as Cdk6 (Figure S5A). Despite this redundancy, Cdk6-deficient neutrophils were impaired in NET production in response to both PMA and *C. albicans* hyphae (Figures 5H and S5C). We obtained similar results with bone marrow-purified neutrophils (Figure S5D). The oxidative burst was unaffected in the knockout animals (Figure 5I), similar to the result with the CDK4/6 inhibitor. There was no difference in peritoneal neutrophil maturity between the two genotypes, as revealed by expression level of the surface marker Ly6G (Figure S5E) and nuclear morphology (Figure S5F). Likewise, we observed no difference in cytokine production (Figure 5J), indicating that Cdk6 deficiency specifically affects NET production, rather than generally modulating inflammatory pathways.

Cdk6 Is Required for Antifungal Defense *In Vivo*

To test the effect of Cdk6 and NET deficiency in infections, we used the murine *C. albicans* sepsis model, which closely reflects the human disease (Spellberg et al., 2005). In this model, *C. albicans* colonizes the kidneys leading to renal failure (Spellberg et al., 2005). The host anti-*Candida* response is mediated primarily by neutrophils (Fulurija et al., 1996), making this a good model for investigating the effect of Cdk6 and NET deficiency on immunity. Mice were intravenously injected with live *C. albicans* and monitored over the course of the infection. Cdk6$^{-/-}$ animals lost weight more rapidly than WT animals (Figure 6A) and also succumbed to the disease more rapidly than WT animals (Figure 6B). Nox2-deficient animals, which are similarly impaired in NET production, also showed reduced survival in response to *C. albicans* challenge (Figure 6B).

We next infected mice with a sublethal dose of *C. albicans* and compared fungal loads in the kidneys 5 days post-infection. We found a strikingly elevated *C. albicans* fungal load in knockout animals (Figure 6C). This effect was not due to differences in peripheral blood counts of neutrophils (Figure S6A) or other immune cells (Figure S5C). Cdk6 was previously implicated in regulating cytokine production (Handschick et al., 2014), but we found equivalent, or even elevated numbers of neutrophils infiltrating the kidneys of Cdk6$^{-/-}$ animals on day 5 post-infection (Figure S6B), indicating that migratory capacity was unaffected. The higher rates of neutrophil accumulation in knockout mice was likely a reflection of higher fungal burdens in these animals. Furthermore, bone marrow-derived macrophages from WT and Cdk6 null mice produced pro- and anti-inflammatory mediators at similar rates (Figure S6D).

Consistent with previous descriptions of sublethal *C. albicans* infections (Fisher et al., 2011), histological analysis of infected kidneys demonstrated that, 5 days post-infection, the fungus produced hyphal filaments, which are associated with tissue destruction, and that these hyphae were collecting in excretory lesions in the papillae of the renal pelvis (Figure 6D). Immunofluorescence analysis revealed that hyphal masses were more abundant in knockout animals: 90% of Cdk6$^{-/-}$ mice had detectable hyphae in the renal papillae, compared with 25% of WT mice.

Cdk6 is broadly expressed in hematopoietic and some non-hematopoietic mouse tissues (Tigan et al., 2015), so its contribution to proper immune defenses could derive from non-myeloid cell activity. To investigate if Cdk6 is required in neutrophils, we restored expression of the kinase in knockout animals by breeding Cdk6$^{-/-}$ mice with animals expressing Cre recombinase (Cre) under the control of a lysozyme M promoter (LysM-Cre). This driver leads to expression of Cre in cells of the myeloid lineage, including neutrophils, monocytes, and macrophages. Expression of Cre in neutrophils led to excision of the floxed STOP cassette and restored Cdk6 to similar levels as in WT mice (Figure S6C). Importantly, genetic rescue of Cdk6 in myeloid cells of knockout mice restored the ability of these mice to mount proper immune responses against *C. albicans* (Figure 6C), demonstrating a role for Cdk6 in antimicrobial defense.

DISCUSSION

Neutrophils are terminally differentiated cells that have stopped proliferating. Indeed, an analysis of cell-cycle proteins demonstrated a downregulation of cyclins and CDKs as neutrophils differentiate from hematopoietic precursors into mature cells (Klausen et al., 2004). Here we show that, despite this

Figure 5. Cdk4/6 Control NET Formation

For a Figure360 author presentation of Figure 5, see https://doi.org/10.1016/j.devcel.2017.10.013#mmc3.

(A) Expression of CDKs in human neutrophils (neutro) and control T cells by western blot analysis. Molecular weights indicated in kDa.

(B) Left: image showing subcellular localization of CDK6 in naive and PMA-stimulated human neutrophils. DNA is shown in blue and CDK6 in green. Scale bars, 5 μm. Right: Quantification of enrichment of CDK6 in neutrophil nuclei, n = 3 donors, bars show means and SEM. **p < 0.01, unpaired Student's t test.

(C) Expression of cyclin D in human neutrophils (neutro) and control PLB-985 cells (PLB) by western blot. (A–C) Representative blots or image from three independent experiments with different donors.

(D and E) NET inhibition with the Cdk4/6 inhibitor abemaciclib (LY2835219) (D) and palbociclib (PD-0332991) after 4 hr of PMA or ConA stimulation (E). Combined data from four donors. Graph shows means and SEM.

(F) Oxidative burst in human neutrophils treated with Cdk4/6 inhibitor or vehicle. Representative data from three independent repeats. Bars = mean and SD.

(G) Phagocytosis of *C. albicans* by human neutrophils pretreated with vehicle (DMSO, black), abemaciclib (red), and cytochalasin D (blue), n = 3 donors.

(H) NET formation in WT and Cdk6$^{-/-}$ mouse peritoneal neutrophils after 5 hr of stimulation with PMA or heat-killed *C. albicans* hyphae. n = 4 per group. ****p < 0.0001, ***p < 0.001.

(I) Oxidative burst measured by luminol assay in WT or Cdk6$^{-/-}$ mouse peritoneal neutrophils stimulated with 100 nM PMA. n = 4 mice per group. ns, not significant.

(J) Mip1α production in WT and Cdk6$^{-/-}$ mouse neutrophils (n = 3 per group), in response to LPS (200 ng/mL). (F–J) Graph shows means ± SEM, unpaired Student's t test. See also Figures S4 and S5.

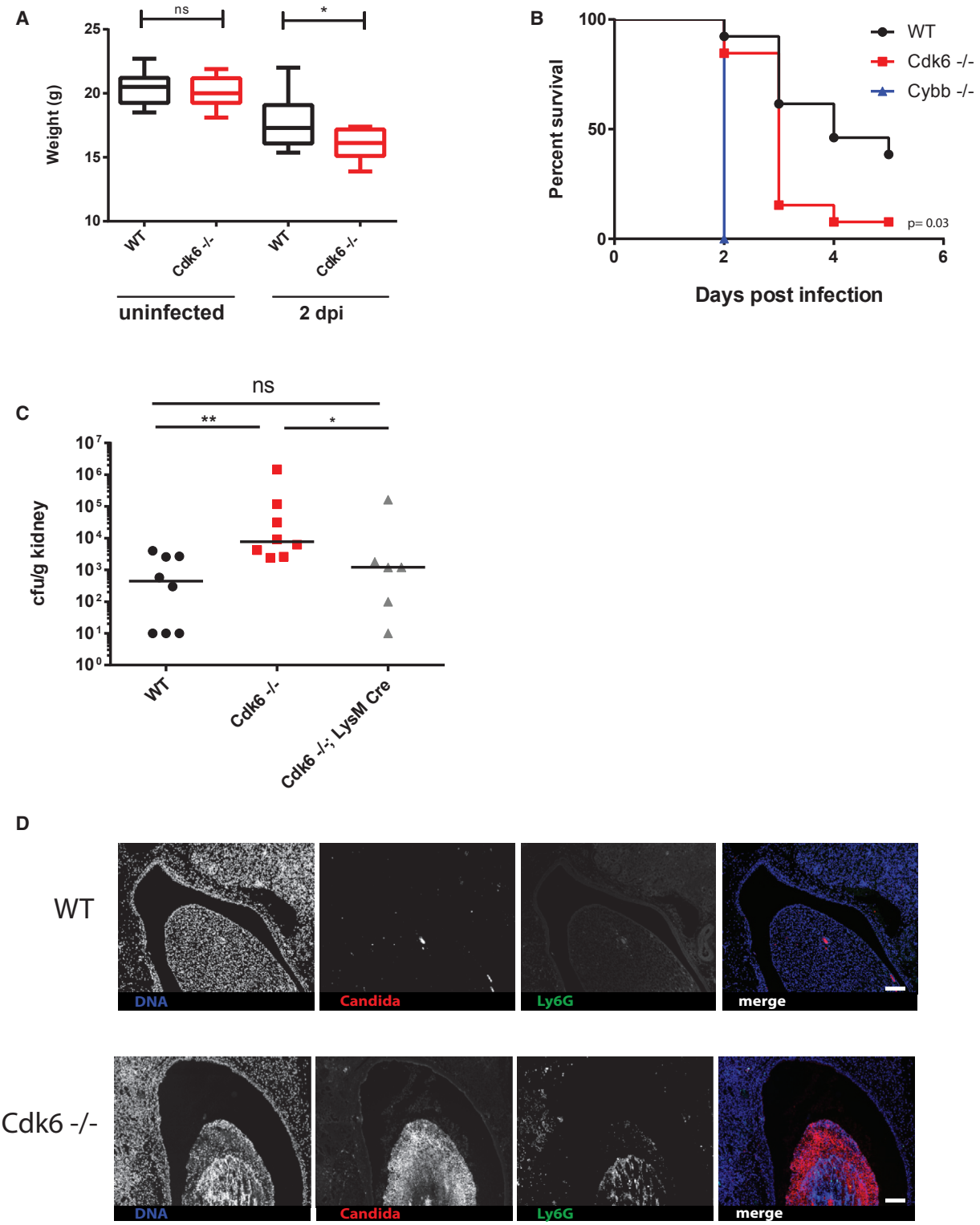

Figure 6. Cdk6 Is Required for Antifungal Defense

(A) Weights (g) of WT and Cdk6$^{-/-}$ mice before and 2 days post-infection with 5 × 10^5 colony-forming unit (CFU) *C. albicans*, boxplots show means; whiskers, 5–95th percentiles; n = 13 mice per group. *p < 0.05, Mann-Whitney U test. ns, not significant.

(B) Kaplan-Meyer survival plot of WT, *Cdk6*$^{-/-}$, and *Nox2 (Cybb)*$^{-/-}$ mice after challenge with 5 × 10^5 CFU *C. albicans*. n = 13. *p < 0.05, log rank (Mantel-Cox) test.

(legend continued on next page)

downregulation, neutrophils can re-activate some aspects of cell-cycle signaling, most notably CDK4/6, upon mitogenic stimulation. We show that NETosis is accompanied by upregulation of Ki-67, phosphorylation of pRb, lamin A/C, and histone H3S10, as well as duplication of centrosomes and nuclear envelope breakdown. Neutrophil activation does not result in DNA synthesis, condensation of chromosomes or cytokinesis, indicating that cell-cycle re-entry is not occurring.

In dividing cells, the cell cycle is tightly controlled and rapidly aborted in response to abnormalities, stress, or disruption of the sequential order of events. Activation of these checkpoints often results in cell death (Malumbres and Barbacid, 2009). It is interesting to speculate that NETotic cell death also results from triggering of one of these checkpoints. For instance, attempted DNA replication without concomitant production of histones arrests the cell cycle in G_2 (Gunesdogan et al., 2014). Furthermore, NET formation also requires production of ROS (Fuchs et al., 2007), which can damage DNA and activate the DNA damage checkpoint in both dividing cells (Malumbres and Barbacid, 2009) and in neutrophils (Harbort et al., 2015). At this point, it is unclear if CDK4/6 promote NETs via cell-cycle signaling or completely unrelated pathways; therefore the involvement of checkpoints also remains speculative.

ROS can also be mitogenic by activating growth factor receptors (Verbon et al., 2012), but, in NETosis, NOX2-derived ROS do not appear to be upstream of cell-cycle signaling, as phosphorylation of pRb and lamin A/C proceeds unchanged in neutrophils from CGD patients. CDK4/6 thus function in a parallel pathway to ROS production; these kinases are necessary but not sufficient for NET formation.

NET formation was inhibited by transduction of a peptide mimic derived from the CDK binding domain of p21, providing an indication that a CDK is involved in the process. p21 is an endogenous cell-cycle inhibitor that blocks CDK activity, just like the peptide mimic employed here. Cells from p21 null mice have higher proliferative capacities (Balomenos et al., 2000) and neutrophils from these mice also exhibited elevated rates of NET formation. p21 knockout mice have been reported to have stronger inflammatory reactions (Martin et al., 2016) and, interestingly, p21 knockout mice also spontaneously develop SLE (Balomenos et al., 2000), a chronic autoimmune disease that has been associated with excessive NET release (Kaplan and Radic, 2012) and accumulation of antibodies against DNA and histones.

Mitogenic signaling in quiescent cells can lead to cell-cycle restart by activating CDK4/6 (Tigan et al., 2015). Consistent with this idea, we show that CDK4/6 are activated upon mitogenic stimulation of neutrophils, and that these kinases regulate NET formation. Our observation that CDK4/6 are the only cell-cycle CDKs expressed in human neutrophils potentially explains the unusual mix of cell-cycle markers induced during NET formation, since these kinases are active in both phosphorylating pRb in G_1 phase, and inducing centrosome separation in M phase (Hussain et al., 2013). It remains unclear, however, if CDK4/6 control NETs via cell-cycle substrates or via targets that are unrelated to cell-cycle control. pRb phosphorylation and centrosome separation could thus simply be markers of CDK4/6 activation, rather than being integral to the mechanism of NET release.

CDK6 is predominantly expressed in blood cells where it plays a role in T cell development and lymphomagenesis (Hu et al., 2009, 2011). It regulates cell-cycle re-entry in certain subsets of hematopoietic precursors (Laurenti et al., 2015; Scheicher et al., 2015), but, despite this, levels of peripheral blood leukocytes, including neutrophils, are normal in Cdk6 knockout mice (Figure S5), probably due to compensation from Cdk4. Alternative roles for Cdk6 as a transcriptional regulator have also been uncovered (Handschick et al., 2014). It is unlikely that Cdk6 regulates NETs via transcriptional regulation, since NET formation is independent of *de novo* gene expression (Sollberger et al., 2016). Furthermore, the fact that ROS and cytokine production, as well as surface marker expression, are unperturbed in $Cdk6^{-/-}$ neutrophils, argues against a defect in differentiation or a general deficiency in inflammatory signaling.

We identify a role for Cdk6 in innate immune defense. Mice lacking this kinase are highly susceptible to infection with the fungal pathogen *C. albicans*. In acute systemic candidiasis, the immune response is predominantly mediated by neutrophils and not by T cell responses, since mice lacking T cells do not show any increase in susceptibility to disease (Cutler, 1976). CDK6 was shown to regulate cytokine production in HeLa cells (Handschick et al., 2014), but we failed to detect a defect in neutrophil recruitment to infected organs. Macrophages, the major producers of cytokines during infections, produced normal levels of these inflammatory mediators despite lacking CDK6. Elevated kidney fungal loads are thus likely a reflection of a defect in neutrophil function, specifically one in NET formation, although the use of the LysM-Cre driver in the rescue experiment means we cannot rule out other impairments in myeloid cells. Cdk6 was shown to regulate macrophage adhesion in response to lipopolysaccharide LPS, and knockout mice are protected against LPS-induced sepsis (Hennessy et al., 2011). This finding is in line with a role for Cdk6 in NET formation, since NETs are also implicated in the pathology of sepsis (Camicia et al., 2014).

NETs are important for immune defense, but are also dysregulated in many autoimmune diseases. Intriguingly, a genetic polymorphism in *CDK6* has been associated with rheumatoid arthritis (Raychaudhuri et al., 2008). CDK6 expression levels are also elevated in various types of cancer, and inhibition of this kinase appears to be a promising new antitumor therapy (Tigan et al., 2015). It is of note that malignancies such as chronic myelogenous leukemia are associated with high levels of NET-induced thrombosis (Demers et al., 2012). The contribution of

(C) *C. albicans* CFU expressed per gram of kidney tissue in WT, $Cdk6^{-/-}$, and conditional rescue $Cdk6^{-/-}$; LysM-Cre^{+} mice, 5 days post-infection with 1×10^5 CFU. Lines indicate median. $^{**}p < 0.01$; $^{*}p < 0.05$ Mann-Whitney U test. ns, not significant.

(D) *C. albicans* (red) and neutrophils (Ly6G, green) in papillae of renal pelvis (visualized by DNA stain/blue) of WT and $Cdk6^{-/-}$ mice, day 5 post-infection. Representative image of nine analyzed kidneys per genotype. Scale bar, 200 μm. See also Figure S6.

CDK6 to cancer may thus be 2-fold: cell-cycle dysregulation contributing to tumorigenesis as well as increased NET formation by myeloid cell precursors leading to thrombosis, the second most common cause of death in cancer patients (Rickles et al., 1992). Use of CDK4/6 inhibitors in cancer therapy may consequently lower rates of thrombosis, but also dampen immune responses in patients.

Interestingly, other instances exist where cell-cycle signaling in postmitotic cells has been linked to disease (Herrup and Yang, 2007). In the brain, neurons can inappropriately re-activate the cell cycle, which leads to cell death just as it does in neutrophils. Cell death resulting from neuron cell-cycle re-entry has been linked to several neurodegenerative diseases, including Alzheimer's disease and amyotrophic lateral sclerosis (Busser et al., 1998; Herrup and Yang, 2007). Dysregulation of cell-cycle proteins in postmitotic neurons and neutrophils can thus be viewed as a unifying disease principle in neurodegenerative and inflammatory disorders.

In summary, NET formation, an antimicrobial form of cell death, is controlled by the activation of the cell-cycle kinases CDK4/6. During infection, lymphocytes activate the cell cycle to rapidly increase their numbers and thus fulfill their memory or cytotoxic functions. We show that, in neutrophils, similar pathways are used for regulating the NETotic cell death program, with essential consequences for immunopathology and defense against pathogens. These findings open up avenues for therapeutic interventions in NET-related diseases.

STAR★METHODS

Detailed methods are provided in the online version of this paper and include the following:

- KEY RESOURCES TABLE
- CONTACT FOR REAGENT AND RESOURCE SHARING
- EXPERIMENTAL MODEL AND SUBJECT DETAILS
  - Human Samples
  - Mice
  - Mouse Infections
  - Cell Line
- METHOD DETAILS
  - Purification of Human Peripheral Blood Neutrophils
  - NET Induction and Quantification
  - Immunofluorescence
  - Transmission Electron Microscopy
  - Western Blotting
  - Microarray Analysis
  - Quantitative Real-Time PCR
  - Peptide Inhibition Experiments
  - EdU Incorporation Assay
  - Mouse NETs
  - Histology
  - Mouse Peripheral Blood Counts
  - ROS Assay
  - Phagocytosis Assay
  - Degranulation Assay
  - Purification of Kidney Immune Infiltrate
- QUANTIFICATION AND STATISTICAL ANALYSIS
- DATA AND SOFTWARE AVAILABILITY

SUPPLEMENTAL INFORMATION

Supplemental Information includes six figures, one table, and one movie and can be found with this article online at https://doi.org/10.1016/j.devcel.2017.10.013.

AUTHOR CONTRIBUTIONS

B.A. and A.Z. conceived and designed the study. B.A., L.K., and C.J.H. performed the laboratory experiments. U.A.A., V.B., and B.A. performed microscopy. B.E.C. analyzed the microarray data. N.D., F.H., and P.H. contributed with reagents/materials. B.A. and A.Z. wrote/drafted and finalized the paper. All authors read and approved the final manuscript.

ACKNOWLEDGMENTS

We thank the blood donors; Alf Herzig and Baerbel Raupach for helpful discussions; and Christian Goosman for transmission electron microscopy. B.A. was supported by an EMBO Long-Term Fellowship; B.E.C. is supported by Sonderforschungsbereich grant SFB-TR84.

Received: August 17, 2016
Revised: July 12, 2017
Accepted: October 9, 2017
Published: November 2, 2017

REFERENCES

Amulic, B., Cazalet, C., Hayes, G.L., Metzler, K.D., and Zychlinsky, A. (2012). Neutrophil function: from mechanisms to disease. Annu. Rev. Immunol. *30*, 459–489.

Balomenos, D., Martin-Caballero, J., Garcia, M.I., Prieto, I., Flores, J.M., Serrano, M., and Martinez, A.C. (2000). The cell cycle inhibitor p21 controls T-cell proliferation and sex-linked lupus development. Nat. Med. *6*, 171–176.

Bedelbaeva, K., Snyder, A., Gourevitch, D., Clark, L., Zhang, X.M., Leferovich, J., Cheverud, J.M., Lieberman, P., and Heber-Katz, E. (2010). Lack of p21 expression links cell cycle control and appendage regeneration in mice. Proc. Natl. Acad. Sci. USA *107*, 5845–5850.

Branzk, N., Lubojemska, A., Hardison, S.E., Wang, Q., Gutierrez, M.G., Brown, G.D., and Papayannopoulos, V. (2014). Neutrophils sense microbe size and selectively release neutrophil extracellular traps in response to large pathogens. Nat. Immunol. *15*, 1017–1025.

Brinkmann, V., Reichard, U., Goosmann, C., Fauler, B., Uhlemann, Y., Weiss, D.S., Weinrauch, Y., and Zychlinsky, A. (2004). Neutrophil extracellular traps kill bacteria. Science *303*, 1532–1535.

Busser, J., Geldmacher, D.S., and Herrup, K. (1998). Ectopic cell cycle proteins predict the sites of neuronal cell death in Alzheimer's disease brain. J. Neurosci. *18*, 2801–2807.

Camicia, G., Pozner, R., and De Larranaga, G. (2014). Neutrophil extracellular traps in sepsis. Shock *42*, 286–294.

Cutler, J.E. (1976). Acute systemic candidiasis in normal and congenitally thymic-deficient (nude) mice. J. Reticuloendothel. Soc. *19*, 121–124.

Demers, M., Krause, D.S., Schatzberg, D., Martinod, K., Voorhees, J.R., Fuchs, T.A., Scadden, D.T., and Wagner, D.D. (2012). Cancers predispose neutrophils to release extracellular DNA traps that contribute to cancer-associated thrombosis. Proc. Natl. Acad. Sci. USA *109*, 13076–13081.

Fisher, J.F., Kavanagh, K., Sobel, J.D., Kauffman, C.A., and Newman, C.A. (2011). *Candida* urinary tract infection: pathogenesis. Clin. Infect. Dis. *52*, S437–S451.

Fuchs, T.A., Abed, U., Goosmann, C., Hurwitz, R., Schulze, I., Wahn, V., Weinrauch, Y., Brinkmann, V., and Zychlinsky, A. (2007). Novel cell death program leads to neutrophil extracellular traps. J. Cell Biol. *176*, 231–241.

Fulurija, A., Ashman, R.B., and Papadimitriou, J.M. (1996). Neutrophil depletion increases susceptibility to systemic and vaginal candidiasis in mice, and

reveals differences between brain and kidney in mechanisms of host resistance. Microbiology *142*, 3487–3496.

Goulvestre, C., Chereau, C., Nicco, C., Mouthon, L., Weill, B., and Batteux, F. (2005). A mimic of p21WAF1/CIP1 ameliorates murine lupus. J. Immunol. *175*, 6959–6967.

Gunesdogan, U., Jackle, H., and Herzig, A. (2014). Histone supply regulates S phase timing and cell cycle progression. Elife *3*, e02443.

Hakkim, A., Fuchs, T.A., Martinez, N.E., Hess, S., Prinz, H., Zychlinsky, A., and Waldmann, H. (2011). Activation of the Raf-MEK-ERK pathway is required for neutrophil extracellular trap formation. Nat. Chem. Biol. *7*, 75–77.

Handschick, K., Beuerlein, K., Jurida, L., Bartkuhn, M., Muller, H., Soelch, J., Weber, A., Dittrich-Breiholz, O., Schneider, H., Scharfe, M., et al. (2014). Cyclin-dependent kinase 6 is a chromatin-bound cofactor for NF-kappaB-dependent gene expression. Mol. Cell *53*, 193–208.

Harbort, C.J., Soeiro-Pereira, P.V., Von Bernuth, H., Kaindl, A.M., Costa-Carvalho, B.T., Condino-Neto, A., Reichenbach, J., Roesler, J., Zychlinsky, A., and Amulic, B. (2015). Neutrophil oxidative burst activates ATM to regulate cytokine production and apoptosis. Blood *126*, 2842–2851.

Heald, R., and McKeon, F. (1990). Mutations of phosphorylation sites in lamin A that prevent nuclear lamina disassembly in mitosis. Cell *61*, 579–589.

Hennessy, E.J., Sheedy, F.J., Santamaria, D., Barbacid, M., and O'Neill, L.A.J. (2011). Toll-like receptor-4 (TLR4) down-regulates microRNA-107, increasing macrophage adhesion via cyclin-dependent kinase 6. J. Biol. Chem. *286*, 25531–25539.

Herrup, K., and Yang, Y. (2007). Cell cycle regulation in the postmitotic neuron: oxymoron or new biology? Nat. Rev. Neurosci. *8*, 368–378.

Hu, M.G., Deshpande, A., Enos, M., Mao, D., Hinds, E.A., Hu, G.F., Chang, R., Guo, Z., Dose, M., Mao, C., et al. (2009). A requirement for cyclin-dependent kinase 6 in thymocyte development and tumorigenesis. Cancer Res. *69*, 810–818.

Hu, M.G., Deshpande, A., Schlichting, N., Hinds, E.A., Mao, C., Dose, M., Hu, G.-F., Van Etten, R.A., Gounari, F., and Hinds, P.W. (2011). CDK6 kinase activity is required for thymocyte development. Blood *117*, 6120–6131.

Hussain, M.S., Baig, S.M., Neumann, S., Peche, V.S., Szczepanski, S., Nurnberg, G., Tariq, M., Jameel, M., Khan, T.N., Fatima, A., et al. (2013). CDK6 associates with the centrosome during mitosis and is mutated in a large Pakistani family with primary microcephaly. Hum. Mol. Genet. *22*, 5199–5214.

Kaplan, M.J., and Radic, M. (2012). Neutrophil extracellular traps: double-edged swords of innate immunity. J. Immunol. *189*, 2689–2695.

Kenny, E.F., Herzig, A., Kruger, R., Muth, A., Mondal, S., Thompson, P.R., Brinkmann, V., Von Bernuth, H., and Zychlinsky, A. (2017). Diverse stimuli engage different neutrophil extracellular trap pathways. Elife *6*, https://doi.org/10.7554/eLife.24437.

Klausen, P., Bjerregaard, M.D., Borregaard, N., and Cowland, J.B. (2004). End-stage differentiation of neutrophil granulocytes in vivo is accompanied by up-regulation of p27kip1 and down-regulation of CDK2, CDK4, and CDK6. J. Leukoc. Biol. *75*, 569–578.

Klein, C. (2011). Genetic defects in severe congenital neutropenia: emerging insights into life and death of human neutrophil granulocytes. Annu. Rev. Immunol. *29*, 399–413.

Laurenti, E., Frelin, C., Xie, S., Ferrari, R., Dunant, C.F., Zandi, S., Neumann, A., Plumb, I., Doulatov, S., Chen, J., et al. (2015). CDK6 levels regulate quiescence exit in human hematopoietic stem cells. Cell Stem Cell *16*, 302–313.

Leitch, A.E., Lucas, C.D., Marwick, J.A., Duffin, R., Haslett, C., and Rossi, A.G. (2012). Cyclin-dependent kinases 7 and 9 specifically regulate neutrophil transcription and their inhibition drives apoptosis to promote resolution of inflammation. Cell Death Differ. *19*, 1950–1961.

Li, P., Li, M., Lindberg, M.R., Kennett, M.J., Xiong, N., and Wang, Y. (2010). PAD4 is essential for antibacterial innate immunity mediated by neutrophil extracellular traps. J. Exp. Med. *207*, 1853–1862.

Lim, S., and Kaldis, P. (2013). Cdks, cyclins and CKIs: roles beyond cell cycle regulation. Development *140*, 3079–3093.

Losman, M.J., Fasy, T.M., Novick, K.E., and Monestier, M. (1992). Monoclonal autoantibodies to subnucleosomes from a MRL/Mp(-)+/+ mouse. Oligoclonality of the antibody response and recognition of a determinant composed of histones H2A, H2B, and DNA. J. Immunol. *148*, 1561–1569.

Malumbres, M., and Barbacid, M. (2009). Cell cycle, CDKs and cancer: a changing paradigm. Nat. Rev. Cancer *9*, 153–166.

Malumbres, M., Sotillo, R., Santamaria, D., Galan, J., Cerezo, A., Ortega, S., Dubus, P., and Barbacid, M. (2004). Mammalian cells cycle without the D-type cyclin-dependent kinases Cdk4 and Cdk6. Cell *118*, 493–504.

Mantovani, A., Cassatella, M.A., Costantini, C., and Jaillon, S. (2011). Neutrophils in the activation and regulation of innate and adaptive immunity. Nat. Rev. Immunol. *11*, 519–531.

Mardin, B.R., and Schiebel, E. (2012). Breaking the ties that bind: new advances in centrosome biology. J. Cell Biol. *197*, 11–18.

Martin, C., Ohayon, D., Alkan, M., Mocek, J., Pederzoli-Ribeil, M., Candalh, C., Thevenot, G., Millet, A., Tamassia, N., Cassatella, M.A., et al. (2016). Neutrophil-expressed p21/waf1 favors inflammation resolution in *Pseudomonas aeruginosa* infection. Am. J. Respir. Cell Mol. Biol. *54*, 740–750.

Martinod, K., and Wagner, D.D. (2014). Thrombosis: tangled up in NETs. Blood *123*, 2768–2776.

Metzler, K.D., Goosmann, C., Lubojemska, A., Zychlinsky, A., and Papayannopoulos, V. (2014). A myeloperoxidase-containing complex regulates neutrophil elastase release and actin dynamics during NETosis. Cell Rep. *8*, 883–896.

Meyerson, M., and Harlow, E. (1994). Identification of G1 kinase activity for cdk6, a novel cyclin D partner. Mol. Cell. Biol. *14*, 2077–2086.

Papayannopoulos, V., Metzler, K.D., Hakkim, A., and Zychlinsky, A. (2010). Neutrophil elastase and myeloperoxidase regulate the formation of neutrophil extracellular traps. J. Cell Biol. *191*, 677–691.

Park, J., Wysocki, R.W., Amoozgar, Z., Maiorino, L., Fein, M.R., Jorns, J., Schott, A.F., Kinugasa-Katayama, Y., Lee, Y., Won, N.H., et al. (2016). Cancer cells induce metastasis-supporting neutrophil extracellular DNA traps. Sci. Transl. Med. *8*, 361ra138.

Parker, H., Dragunow, M., Hampton, M.B., Kettle, A.J., and Winterbourn, C.C. (2012). Requirements for NADPH oxidase and myeloperoxidase in neutrophil extracellular trap formation differ depending on the stimulus. J. Leukoc. Biol. *92*, 841–849.

Raychaudhuri, S., Remmers, E.F., Lee, A.T., Hackett, R., Guiducci, C., Burtt, N.P., Gianniny, L., Korman, B.D., Padyukov, L., Kurreeman, F.A., et al. (2008). Common variants at CD40 and other loci confer risk of rheumatoid arthritis. Nat. Genet. *40*, 1216–1223.

Rickles, F.R., Levine, M., and Edwards, R.L. (1992). Hemostatic alterations in cancer patients. Cancer Metastasis Rev. *11*, 237–248.

Rousseau, D., Cannella, D., Boulaire, J., Fitzgerald, P., Fotedar, A., and Fotedar, R. (1999). Growth inhibition by CDK-cyclin and PCNA binding domains of p21 occurs by distinct mechanisms and is regulated by ubiquitin-proteasome pathway. Oncogene *18*, 4313–4325.

Scheicher, R., Hoelbl-Kovacic, A., Bellutti, F., Tigan, A.S., Prchal-Murphy, M., Heller, G., Schneckenleithner, C., Salazar-Roa, M., Zochbauer-Muller, S., Zuber, J., et al. (2015). CDK6 as a key regulator of hematopoietic and leukemic stem cell activation. Blood *125*, 90–101.

Sollberger, G., Amulic, B., and Zychlinsky, A. (2016). Neutrophil extracellular trap formation is independent of de novo gene expression. PLoS One *11*, e0157454, eCollection 2016.

Spellberg, B., Ibrahim, A.S., Edwards, J.E., Jr., and Filler, S.G. (2005). Mice with disseminated candidiasis die of progressive sepsis. J. Infect. Dis. *192*, 336–343.

Swamydas, M., Luo, Y., Dorf, M.E., and Lionakis, M.S. (2015). Isolation of mouse neutrophils. Curr. Protoc. Immunol. *110*, 3.20.1–3.20.15.

Tigan, A.S., Bellutti, F., Kollmann, K., Tebb, G., and Sexl, V. (2015). CDK6 – a review of the past and a glimpse into the future: from cell-cycle control to transcriptional regulation. Oncogene *35*, 3083–3091.

Verbon, E.H., Post, J.A., and Boonstra, J. (2012). The influence of reactive oxygen species on cell cycle progression in mammalian cells. Gene *511*, 1–6.

Warnatsch, A., Ioannou, M., Wang, Q., and Papayannopoulos, V. (2015). Inflammation. Neutrophil extracellular traps license macrophages for cytokine production in atherosclerosis. Science *349*, 316–320.

Wong, S.L., Demers, M., Martinod, K., Gallant, M., Wang, Y., Goldfine, A.B., Kahn, C.R., and Wagner, D.D. (2015). Diabetes primes neutrophils to undergo NETosis, which impairs wound healing. Nat. Med. *21*, 815–819.

STAR★METHODS

KEY RESOURCES TABLE

REAGENT or RESOURCE	SOURCE	IDENTIFIER
Antibodies		
Ki67	Abcam	ab16667, RRID: AB_302459
α/β Tubulin	Cell Signaling	Cat. No. 2148, RRID: AB_2288042
pericentrin	Abcam	ab4448, RRID: AB_304461
Lamin A/C phospho-ser392 (immunofluorescence)	Biorbyt	orb99257
Cdk6 (for human detections)	Santa Cruz	Cat. No. 177 (C-21) RRID: AB_631225
Cdk6 (for mouse detections)	Abcam	ab54576, RRID: AB_940952
Elastase	LsBio	B24-244
γ tubulin	Thermo	MA1-19421, RRID: AB_1075282
anti-chromatin (reacts with a complex of Histone 2A, Histone 2B and DNA)	Monestier lab	Losman et al., 1992
Cdk4 (for human detections)	Abcam	EPR4513, RRID: AB_10861376
Cdk4 (for mouse detections)	Genetex	GTX102993, RRID: AB_1949951
CCND1	Santa Cruz	sc-753, RRID: AB_2070433
CCND2	Santa Cruz	sc-593, RRID: AB_2070794
CCND3	Cell Signaling	2936, RRID: AB_10698739
CCNE1	Cell Signaling	HE12, RRID: AB_2071200
CCNE2	Abnova	10197, RRID: AB_1671803
CCNB1	Cell Signaling	4138, RRID: AB_2072132
CCNA2	Cell Signaling	BF683, RRID: AB_2071958
CDK2	Cell Signaling	78B2, RRID: AB_10695594
CDK7	Thermo	PA5-34791, RRID: AB_2552143
phospho-Lamin A/C S22	Cell Signaling	2026, RRID: AB_2136155
Lamin A/C	Cell Signaling	2032, RRID: AB_2136278
phospho histone H3 S10	Cell Signaling	9701, RRID: AB_331535
phospho pRb S780	Cell Signaling	9307, RRID: AB_330015
GAPDH	Cell Signaling	2118, RRID: AB_561053
Bacterial and Virus Strains		
Candida albicans	Urban lab, Umea University	SC5314
Biological Samples		
Human blood	This study	N/A
Chemicals, Peptides, and Recombinant Proteins		
Abemaciclib	Selleck	LY2835219
Ribociclib	Selleck	PD-0332991
SYTO Green	Thermo Fisher	S7575
SYTOX Orange	Thermo Fisher	S11368
P21inh peptide Ac-YGRKKRRQRRRRERWNFDFVTETPLEGDFAW-NH2	Peptide 2.0 Inc	N/A
P21 ctrl peptide Ac-YGRKKRRQRRRLWARDENDEVFRWFTPEFGT-NH2	Peptide 2.0 inc	N/A
Deposited Data		
Microarray data	GEO repository	GSE103755
Experimental Models: Cell Lines		
PLB985	Mary Dinauer, University of Washington	CVCL_2162

(*Continued on next page*)

Continued		
REAGENT or RESOURCE	SOURCE	IDENTIFIER
Experimental Models: Organisms/Strains		
Cdk6 knockout mouse	Hinds lab, Tufts University	B6.129S4-Cdk6^{tm1}/J
P21 knockout kouse	Jackson labs	B6.129S6(Cg)-*Cdkn1a*^{tm1Led}/J
LysM-Cre transgenic mouse	Jackson labs	B6.129P2-*Lyz2*$^{tm1(cre)Ifo}$/J
Oligonucleotides		
β2-microglobulin F 5'-CTCCGTGGCCTTAGCTGTG-3'	Sigma	N/A
β2-microglobulin R 5'-TTTGGAGTACGCTGGATAGCCT-3'	Sigma	N/A
Software and Algorithms		
ImageJ	imagej.net	N/A

CONTACT FOR REAGENT AND RESOURCE SHARING

Further information and requests for reagents should be directed to and will be fulfilled by the Lead Contact, Arturo Zychlinsky (zychlinsky@mpiib-berlin.mpg.de).

EXPERIMENTAL MODEL AND SUBJECT DETAILS

Human Samples

Our study was conducted in accordance with the Helsinki Declaration. Blood donations from healthy donors (male and female, ages 23-53) and CGD patient (male, age 23) were collected after obtaining informed consent. Information on sample size can be found in the figure legends. Histopathological samples were collected anonymously from diagnostic biopsies and autopsies, therefore sex and age reporting is not possible. Both blood and pathology sample collection was approved by the ethical committee of Charité University Hospital, Berlin, Germany.

Mice

Mouse breeding and experiments were approved by the Berlin state authority *Landesamt für Gesundheit und Soziales*. Animals were bred locally at the Max Planck Institute for Infection Biology. They were housed in approved specific pathogen free (SPF) conditions, maintained on a 12-hour light/dark cycle and fed *ad libitum*. Cdk6$^{-/-}$ mice (B6.129S4-Cdk6^{tm1}/J) were generated by a knock-in approach (Hu et al., 2009) and obtained from the Hinds laboratory. They were bred homozygous. p21$^{-/-}$ mice, generated in the Leder lab (B6.129S6(Cg)-*Cdkn1a*^{tm1Led}/J) were obtained from Jackson laboratory and were bred homozygous. For conditional rescue of Cdk6 in myeloid cells, cdk6$^{-/-}$ mice were crossed with LysM- Cre mice (B6.129P2-*Lyz2*$^{tm1(cre)Ifo}$/J), obtained from Jackson laboratory. Experiments were carried out with male and female sex- and age-matched 8-12 week old mice that were confirmed to be infection free and had not been exposed to any previous procedures. For estimation of group size we used the software nQuery. Experimenters were not blinded to animal genotype. For group sizes and statistical tests please see figure legends.

Mouse Infections

C. albicans strain SC5314 was grown as an overnight culture in YPD medium at 30°C with shaking. For lung infections, 10^6 cfu in PBS were delivered via the oral-tracheal route into 8 week old female wild-type C57B6 mice (n=6). Mice were sacrificed and lungs were removed 18 hours later and fixed in 2% PFA.

For disseminated candidiasis, two different doses were used: for survival experiments, animals were injected intravenously (i.v.) with $5x10^5$ cfu and monitored daily. For kidney fungal load, renal histology and immune cell infiltration assays, 8 week old female mice were injected i.v. with $1x10^5$ cfu. After 5 days, animals were sacrificed and kidneys were removed. One kidney was homogenized in a Precellys Evolution bead homogenizer (Bertin technologies) for plating and cfu determination and the other was processed for FACS analysis. For group sizes and statistical tests please see figure legends.

Cell Line

PLB-985 cells (female; RRID:CVCL_2162) were kindly donated by Dr. Mary Dinauer. They were cultured according to standard protocols in RPMI medium with 10% FCS, glutamine and antibiotics. Cells were used exclusively for controls or as a reference. They were not checked for contamination with mycoplasma or with other cell lines. Synchronization in G2 phase was achieved by incubating cells in presence of 10 μM RO3306 for 14 hours, followed by washing and reseeding in normal medium.

METHOD DETAILS

Purification of Human Peripheral Blood Neutrophils

Venous blood was collected into EDTA tubes (S-Monovette, Sarstedt), layered on Histopaque 1119 (Sigma-Aldrich) and centrifuged for 20 min at 800 × *g*. The plasma and upper layers consisting mainly of lymphocytes and monocytes were discarded (or collected for T cell purification). The neutrophil-rich layer was collected, leaving the red blood cells on the bottom of the tube. Neutrophils were washed in PBS, and further fractionated on a discontinuous Percoll (Pharmacia) gradient consisting of layers with densities of 1105 g/ml (85%), 1100 g/ml (80%), 1093 g/ml (75%), 1087 g/ml (70%), and 1081 g/ml (65%). After centrifugation for 20 min at 800 × *g*, the interface between the 80% and 85% Percoll layers was collected and washed with PBS. Neutrophil purity was determined to be > 95% by FACS.

NET Induction and Quantification

Human NETs were induced in culture medium consisting of RPMI supplemented with HEPES (10 mM) and 0.05% human serum albumin (HSA, Grifols), with 50 nM PMA (Sigma), 50 μg/ml ConA (Sigma), 50 μg/ml PHA (Sigma) or live *C. albicans* (previously opsonized in human serum) at a multiplicity of infection (MOI) of 5. Cells were stimulated with mitogens for 4 hours and with *C. albicans* for 2 hours.

NETs were enumerated using a SYTO/SYTOX staining technique. The cell impermeable SYTOX orange dye (1 μM, Thermofisher) was used to detect NETs. SYTO green, a cell-permeable DNA dye (250 nM, Thermofisher), was used to determine the total number of cells. Images were taken on a Leica DM IRBE inverted microscope. Percentage of NET release was calculated by dividing the number of SYTOX positive cells by the number of SYTO positive cells. For studies with chemical inhibitors, cells were plated directly into culture medium containing the inhibitors. Preincubation with Abemaciclib (LY2835219, Selleck) and Palbociclib (Selleck) was for 30 min at the indicated concentrations. Stock solutions of inhibitors were made by dissolving in DMSO and stored for one week at room temperature after which they were discarded.

Immunofluorescence

Neutrophils were fixed on uncoated glass coverslips with 2% paraformaldehyde (PFA), permeabilized for 5 minutes with 0.5% Triton X-100, and then blocked at room temperature for 30 minutes in 1% bovine serum albumin, 5% normal donkey serum, and 3% cold-water fish gelatin (Sigma-Aldrich). To promote attachment of unstimulated cells, neutrophils were first plated for 5 minutes in RPMI without human serum albumin, after which culture medium was added (RPMI with 0.05% HSA). Primary antibodies used were: anti-Ki67 (Abcam SP6), anti-α/β Tubulin (Cell Signaling Technology [CST]), anti-pericentrin (Abcam), anti- Lamin A/C phospho-ser392 (Biorbyt), anti-Cdk6 (Santa Cruz, C-21), anti-elastase (EMD), anti-γ tubulin (Thermo) and anti-chromatin (reacts with a complex of Histone 2A, Histone 2B and DNA, (Losman et al., 1992)). Samples were stained with primary antibodies for 1h at 37°C in blocking buffer, followed by secondary antibodies conjugated to Alexa Fluor 488 or 568 (Invitrogen) together with Hoechst 33342. Coverslips were mounted in Mowiol and images were taken with a Leica SP8 confocal microscope.

Transmission Electron Microscopy

Cells were fixed with 2.5% glutaraldehyde, postfixed with 1% osmiumtetroxide, contrasted with uranylacetate and tannic acid, dehydrated and embedded in Polybed (Polysciences). Specimens were then cut at 60 nm and contrasted with lead citrate. Analysis was carried out on a Leo 906E transmission electron microscope (Oberkochen).

Western Blotting

Protein immunoblotting was performed as previously described (Harbort et al., 2015), with lysates prepared directly in hot SDS loading dye. Primary antibodies used were as follows: anti-CDK6 (Santa Cruz, c-21 [for detecting human protein]), anti-Cdk6 (Abcam ab54576, [for detecting mouse protein]), anti-CDK4 (Abcam EPR4513 [for detecting human protein]), anti-Cdk4 (Genetex GTX102993 [for detecting mouse protein]), anti-CCND1, CCND2, CCND3 (Santa Cruz), anti-CCNE1 (CST HE12), anti-CCNE2 (Abnova 10197), anti-CCNA2 (CST BF683), anti-CCNB1 (CST 4138), anti-CDK1 (Abcam, clone A17), anti-CDK2 (CST 78B2), anti-CDK7 (Thermo Fisher PA5-34791), anti-phospho-Lamin A/C (S22 [CST]), anti-Lamin A/C (CST), anti-phospho histone H3 (S10 [CST]), anti-Histone H3 (CST), anti-phospho pRb (S780 [CST D59B7]), anti-pRb (CST) anti-Ki67 (Abcam SP6) and anti-GAPDH (CST).

Microarray Analysis

RNA from 8 healthy donors was isolated using RNeasy mini kit (Qiagen) and labeled with the Fluorescent Linear Amplification Kit (Agilent Technologies) according to manufacturer's instructions before hybridization to whole-genome 4×44k human expression arrays (Agilent). Data analysis was performed using the limma R package. Expression values were background-corrected followed by quantile normalization between samples.

Quantitative Real-Time PCR

RNA was isolated with RNeasy mini kit (Qiagen). cDNA was made using High-capacity RNA-to-cDNA kit (Applied Biosystems) according to manufacturer's protocol. qPCR was performed on StepOnePlus Real-Time PCR System with 2x Fast SYBR Green master mix (Applied Biosystems). The housekeeping gene

β2-microglobulin (F 5'-CTCCGTGGCCTTAGCTGTG-3' and

R 5'-TTTGGAGTACGCTGGATAGCCT-3') was used as an internal control for relative standard curves. All other cDNAs were amplified with Quantitect primer (Qiagen). Data were analyzed using StepOne software.

Peptide Inhibition Experiments

Tat conjugated peptides were synthesized by Peptide 2.0 Inc (Chantilly, VA, USA). p21inh, corresponding to amino acids 46–65 of the p21 protein: Ac-YGRKKRRQRRRRERWNFDFVTETPLEGDFAW-NH2; p21ctrl: Ac-YGRKKRRQRRRLWARDENDEVFRWFT PEFGT-NH2. Neutrophils were incubated with 20 μM of peptides for 1 hour in Hank's Balanced Salt Solution (HBSS) without magnesium or calcium ions, with orbital rotation. Subsequently, the cells were diluted 1:20 in culture medium, plated and stimulated with PMA.

EdU Incorporation Assay

DNA synthesis was monitored using the Click-iT EdU Alexa Fluor 488 Imaging Kit (Thermo Fisher) as per manufacturer's instructions. Neutrophils, T cells or HEK cells were incubated with EdU for 20 min before stimulation (in the case of neutrophils and T cells). Control human T cells were purified from peripheral blood mononuclear cell (PBMC) fractions. After separation on Histopaque 1119 (Sigma-Aldrich), PBMCs were stimulated with PHA, incubated for 5 days and then restimulated with 20 ng/ml PMA and 200 ng/ml ionomycin to induce proliferation in the presence of EdU.

Mouse NETs

Mouse peritoneal neutrophils were elicited with casein (Sigma) and purified on a Percoll gradient as previously published (Swamydas et al., 2015). Mouse bone marrow neutrophils were purified as previously described (Sollberger et al., 2016). Cells were stimulated in RPMI supplemented with 1% DNase$^{-/-}$ mouse serum and 100 ng/ml G-CSF (Peprotech) with either PMA (100 nM) or heat killed *C. albicans* hyphae (Sollberger et al., 2016) for the indicated times.

Histology

Human biopsy and autopsy tissue was fixed in formalin and embedded in paraffin. Four micrometer thick paraffin sections were stained using routine Periodic acid–Schiff (PAS) staining or with antibodies against Ki-67 (MiB1, Dako) by using the iView-Ventana diaminobenzidine (DAB) Detection Kit (Ventana) with biotinylated secondary antibodies and DAB visualization of the peroxidase reaction product with a Benchmark XT immunostainer (Ventana).

Mouse lungs and kidneys were fixed in 2% PFA, embedded in paraffin and cut to 5 μm sections.

Immunofluorescence experiments were carried out with anti-Ki67 (Abcam SP6), anti-pericentrin (Abcam), anti-Calgranulin A (S100A8) (produced in-house) and anti- *C. albicans* (Acris BP1006) primary antibodies, followed by Alexa secondary antibodies (Invitrogen).

Microscopy was performed with a Leica SP8 confocal microscope.

Mouse Peripheral Blood Counts

Cell populations in whole blood were identified and quantified by flow cytometry with the following antibodies: anti- CD115 (AF598, eBioscience), anti-Gr-1 (RB6-8C5, Biolegend), anti-CD3 (17A2, BD Bioscience), anti-CD4 (RM4-5, BD Bioscience), CD8a (53-6.7, BD Bioscience), anti-B220 (RA3-6B2, Biolegend). Antibodies were added directly to 100 μL of heparinized whole blood at a 1:200 dilution and incubated at room temperature for 30 minutes. Stained cells were fixed and erythrocytes were lysed simultaneously with 1-step Fix/Lyse solution (Affymetrix eBioscience). AccuCheck Counting beads (Invitrogen) were added to obtain total cell counts. Samples were acquired on a BD LSRFortessa using DIVA software and analyzed by Flowjo (Treestar) software.

ROS Assay

Neutrophils were seeded in 96-well plates at a concentration of $1x10^5$ cells per well in 200 μl medium supplemented with 50 μM luminol and 1.2 units/ml horseradish peroxidase, both from Sigma. After 30 minute incubation at 37°C, cells were stimulated with 100 nM PMA and luminescence was measured over time in a VICTOR Light luminescence counter (Perkin Elmer) and expressed as Relative Light Units (RLU).

Phagocytosis Assay

Green fluorescent protein (GFP)-expressing *C. albicans* strain sc5314 (kind gift of Brendan Cormack) was opsonized with 10% human serum for 20 minutes and incubated with purified human neutrophils. For inhibitor experiments, neutrophils were pretreated with compounds for 30 minutes. Phagocytocis was allowed to proceed for 30 minutes at 37°C with rotation in RPMI supplemented with 0.1% human serum albumin, after which cells were fixed with 2% PFA. Neutrophils were labelled with an anti-CD15 antibody coupled with allophycocyanin (APC). Percentage phagocytosis was determined by FACS analysis of GFP and APC positive cells.

Degranulation Assay

Human neutrophils were stimulated with opsonized zymosan (10 μg/ml) or medium for 2 hours to stimulate degranulation of elastase. Zymosan (Sigma) was opsonized with 10% pooled human serum from 6 donors for 30 minutes at 37°C. Elastase release in supernatants was quantified using the human elastase ELISA kit (Hycult).

Purification of Kidney Immune Infiltrate

Neutrophils in infected kidneys were analyzed as outlined in (Swamydas et al., 2015). Briefly, kidneys were finely sliced with a scalpel and digested for 30 min in the presence of 0.2125 mg/ml Liberase TL (Roche) and 0.1 mg/ml DNase I (Roche). After digestion, kidneys were strained through a 70 μm sieve, red cells were lysed with ACK lysis buffer (Lonza) and the pellet was resuspended in 40% Percoll. This was loaded over 70% Percoll and centrifuged at 872x g for 30 min. Cells were collected from the interface and analyzed by FACS.

QUANTIFICATION AND STATISTICAL ANALYSIS

GraphPad Prism was used to generate graphs and perform all statistical tests. For NET assays, immunofluorescence quantifications, ROS production, phagocytosis and cytokine secretion, graphs show means +/- standard error of the mean and unpaired t test was used for statistical comparisons. Mann-Whitney U test was used for comparing cfu enumeration and neutrophil counts. Survival data were analyzed by the Kaplan-Meier method with Mantel-Cox log-rank testing. Details of statistical analyses for quantifications are in corresponding figure legends, including significance levels, exact n values and what n represents for each experiment.

DATA AND SOFTWARE AVAILABILITY

The values for microarray expression analysis have been deposited in GEO repository as GEO: GSE103755.